JOURNAL OF MATERIALS SCIENCE **38** (2003) 3249–3255

Interaction of iron-chromium alloys containing 10 and 25 mass% chromium with liquid aluminium

Part I *Dissolution kinetics*

K. BARMAK
Department of Materials Science and Engineering, Carnegie Mellon University, Pittsburgh, PA 15213, USA
E-mail: katayun@andrew.cmu.edu
URL: http://neon.mems.cmu.edu/barmak.html

V. I. DYBKOV
Department of Physical Chemistry of Inorganic Materials, Institute for Problems of Materials Science, Kyiv 03180, Ukraine
E-mail: v@dybkov.kiev.ua; dep6@materials.kiev.ua
URL: http://users.i.com.ua/~dybkov/V/index.html

The dissolution process of iron-chromium alloys containing 10 and 25 mass% Cr in an aluminium melt at 700°C is found by the rotating-disc technique to be diffusion-controlled and non-selective. Experimentally determined values of the saturation concentration (solubility) and the dissolution rate constant of iron and chromium in liquid aluminium for the Fe–Cr alloys are presented. Evaluated values of the diffusion coefficients of Fe and Cr across the diffusion boundary layer into the melt are also given.

1. Introduction

All-in-one joining of commercial iron-chromium alloys with aluminium and its alloys encounters considerable difficulties in view of formation of extremely brittle intermetallic layers of low mechanical strength in the joint. By increasing their dissolution rate in the liquid-metal bath, the thickness of these layers can be significantly reduced. To evaluate the extent of such a reduction, experimental data on the dissolution kinetics of the solid-alloy base in the aluminium melt are clearly needed. This process is characterized by the saturation concentrations (solubilities) of the alloy components in the liquid phase and their dissolution rate constants. In the case of a binary alloy, the dissolution rate constants can be either identical for both components (non-selective dissolution) or different (selective dissolution).

Fe–Cr alloy-to-aluminium joining as well as coating of the alloy surface with aluminium to improve its high-temperature resistance to oxidation are to be carried out at a temperature not too different from the melting point of aluminium. Temperatures in the vicinity of 700°C are practicable. In Part I of this paper, the results of our investigation of the dissolution process of iron-chromium alloys containing 10 and 25 mass% Cr in an aluminium melt at 700°C are presented. Experimental data on phase identity, chemical composition, morphology and growth kinetics of the intermetallic-compound layers at the alloy-aluminium interface, with emphasis on the effect of dissolution on the layer-growth rate, will be discussed in Part II.

2. Experimental procedure

2.1. Materials and alloy preparation

Powder of carbonyl iron (99.98 mass% Fe) and platelets of electrolytic-grade chromium (99.98 mass% Cr) were used for the preparation of the Fe–Cr alloys. High-purity aluminium (99.995 mass% Al) was employed as the melt material. The Fe–Cr alloys were prepared in a conventional arc-melting furnace with a non-consumable tungsten electrode and a water-cooled copper mould under argon, and then cast into 13 mm inner diameter (i.d.) and 100 mm high massive copper crucibles to ensure rapid crystallization of the melt. By inverting the ingots between melts, and re-melting five or six times, homogeneous alloys could readily be obtained.

2.2. Fe–Cr specimens and their characterization

Cylindrical specimens, 11.28 ± 0.01 mm diameter and approximately 6 mm high, were machined from the 13 mm diameter Fe–Cr alloy rods. The disc surfaces were then ground flat and polished mechanically. Prior to the start of experiments aimed at measuring the dissolution rate constant, the alloy specimen was rinsed in ethanol and dried. It was then pressed into a 16 mm

TABLE I Chemical composition of the Fe–Cr alloy samples

Nominal alloy composition (mass%)		Sample number	Content of elements (mass%)					
			CA		EPMA			
					US		UA	
Fe	Cr		Fe	Cr	Fe	Cr	Fe	Cr
90	10	2	90.1	10.1	89.9	10.1	89.6	10.4
		3	90.0	10.1	90.6	9.4	89.5	10.5
		3B	90.3	9.7	89.5	10.5	89.9	10.1
		4B	89.7	10.0	90.1	9.9	89.7	10.3
75	25	1B	75.2	24.9	75.4	24.6	74.7	25.3
		2	75.1	25.0	74.8	25.2	74.5	25.5
		2B	74.9	25.0	74.5	25.5	75.7	24.3
		4	75.5	24.6	75.5	24.5	74.3	25.7

Note: CA = chemical analysis, EPMA = electron probe microanalysis, US = United States, UA = Ukraine.

diameter high-purity graphite tube to protect its lateral surface from attack by the liquid aluminium. As a result, only the disc surface, 1 cm^2 in area, contacted the aluminium melt. However, when determining the saturation concentrations of iron and chromium in liquid aluminium, a greater specimen surface was needed to shorten the experiment duration. In this case, cylindrical alloy specimens with unprotected lateral surfaces were employed. The initial surface area of these specimens exposed to the liquid metal was approximately 2.75 cm^2.

Chemical compositions of the Fe–Cr alloy samples were found to correspond closely to the nominal values of 10 and 25 mass% Cr (Table I). Alloy compositions were measured by chemical analysis (CA) as well as by electron probe microanalysis (EPMA) and are given in Table I. The EPMA experiments were carried out in both the United States (US) and Ukraine (UA) using microanalyzers JEOL Superprobe 733 and CAMECA Camebax SX50.

X-ray diffraction studies revealed that both Fe–Cr samples were body centered cubic α-phase (ferrite), as shown in Table II [1, 2]. This equally applies to room temperature and the temperature chosen in this investigation, 700°C, since, according to the equilibrium phase diagram of the Fe–Cr binary system, the α-to-γ transition should only take place above 830°C [3].

2.3. Methods

The dissolution runs were carried out by the rotating-disc technique using a rapid-quenching device described in detail elsewhere [4]. The experimental procedure did not differ considerably from that described in previous works [5, 6]. Briefly, it was as follows.

First, a flux consisting of alkali halides and other salts was melted in a 26 mm i.d. alumina crucible. Its melting began at about 350°C. The flux was used both to protect the aluminium melt from oxidation and to preheat the Fe–Cr specimen to the required temperature. Then, pieces of aluminium (24 g) were melted under the flux. At 700°C, this amount corresponded to a volume of 10 cm^3 of liquid aluminium. After the temperature had equilibrated, the specimen, rotating at the required angular speed of 54.0 rad s^{-1} for determining the saturation concentration or 24.0 rad s^{-1} for determining the dissolution rate constant, was lowered from its position in the middle of the flux column, where it was being preheated to the investigation temperature at a lower rotational speed of 6.45 rad s^{-1}, into the bulk of the aluminium melt.

The lowering of the Fe–Cr specimen marked the start of the dissolution run. The specimen was allowed to rotate in liquid aluminium for a predetermined period of time in the range of 300–5400 s. At the end of the run, the sample was lifted above the aluminium-melt surface and rapidly cooled in a water bath. The temperature of the liquid phase was maintained to within ±2°C, except at the start of the run when its deviations were somewhat larger (up to ±5°C). Temperature measurements were carried out using Pt–Pt(Rh) and chromel-alumel thermocouples.

After cooling the (Fe–Cr) + Al bimetallic specimen to room temperature, the major portion of the Al–Fe–Cr alloy adhering to the Fe–Cr alloy base was removed mechanically. The remainder was dissolved in a 20% aqueous solution of NaOH or KOH. The Fe–Cr alloy specimen was then cleaned with a metallic brush, washed with alcohol, dried, and finally weighed to determine its mass loss during dissolution in liquid aluminium.

After the experiments, samples of the Al–Fe–Cr alloys were analysed chemically by photometric methods to find their iron and chromium contents. For this purpose, use was also made of EPMA. The relative error in

TABLE II X-ray diffraction results for Fe–Cr alloy samples. The reflections are designated as *hkl* and the associated interplanar spacings as *d*

	$d_{literature}$ for the α-phase (nm)		$d_{experimental}$ for the Fe–Cr alloy samples (nm)							
			90 mass% Fe–10 mass% Cr				75 mass% Fe–25 mass% Cr			
hkl	[1]	[2]	No. 2[a]	3	3B	4B	No. 1B[a]	2	2B	4
110	0.2027	0.2010	0.2020	0.2020	0.2015	0.2021	0.2020	0.2022	0.2017	0.2023
200	0.1433	0.1428	0.1430	0.1430	0.1429	0.1431	0.1430	0.1430	0.1424	0.1431
211	0.1170	0.1166	0.1170	0.1170	0.1171	0.1171	0.1173	0.1172	0.1170	0.1173
220	0.1013	0.1010	0.1014	0.1015	0.1012	0.1013	0.1016	0.1015	0.1015	0.1014
310	0.0906	0.0904	0.0908	0.0907	0.0907	0.0908	0.0908	0.0909	0.0908	0.0909
222	0.0828	0.0825	0.0828	0.0828	0.0830	0.0828	0.0829	0.0829	0.0830	0.0827

[a]Sample number.

the compositions were on average approximately ±5% for iron and ±8% for chromium.

3. Results and discussion

3.1. Saturation concentrations of iron and chromium for the dissolution of Fe–Cr alloys in liquid aluminium

Under conditions of intensive agitation, the Nernst-Shchukarev equation is known to describe the dissolution process of any solid in a liquid phase (see, for example, [4–7]). Its differential form is

$$\frac{dc}{dt} = k\frac{s}{v}(c_s - c) \tag{1}$$

where c is the instantaneous concentration of the dissolved substance in the bulk of the liquid phase at a time t, c_s is the saturation concentration or solubility at a given temperature, k is the dissolution rate constant, s is the surface area of the solid in contact with the liquid, and v is the volume of the liquid phase. When integrated with the initial condition $c = 0$ at $t = 0$, it becomes

$$c = c_s\left[1 - \exp\left(-\frac{kst}{v}\right)\right] \tag{2}$$

or in another form

$$\ln\frac{c_s}{c_s - c} = k\frac{st}{v}. \tag{3}$$

If the initial concentration of the dissolving substance in the liquid is equal to c_0, then

$$\ln\frac{c_s - c_0}{c_s - c} = k\frac{st}{v}. \tag{4}$$

Equations 1–4 indicate that the process of dissolution of a solid in a liquid is fully characterised by the two quantities, namely, the saturation concentration or solubility, c_s, and the dissolution rate constant, k. At a constant pressure, the former only depends upon temperature. The latter is in addition dependent upon the hydrodynamic conditions of flow of the liquid.

From the above equations, the concentration of the dissolved substance in the liquid is seen to increase with time and to reach its limiting value, c_s, as was the case for Fe–Cr alloys (Fig. 1 and Table III). At 700°C, this limiting value was found to be 2.5 ± 0.2 mass% Fe and 0.28 ± 0.03 mass% Cr for a 90 mass% Fe–10 mass% Cr alloy and 2.2 ± 0.2 mass% Fe and 0.72 ± 0.06 mass% Cr for a 75 mass% Fe–25 mass% Cr alloy. For comparison, the solubility limits of iron and chromium in liquid aluminium in the Al–Fe and Al–Cr binary systems at 700°C are 2.5 mass% and 0.72 mass%, respectively [4, 5]. The former value coincides with the saturation concentration of iron for the 90 mass% Fe–10 mass% Cr alloy, while the latter corresponds to the saturation concentration of chromium for the 75 mass% Fe–25 mass% Cr alloy.

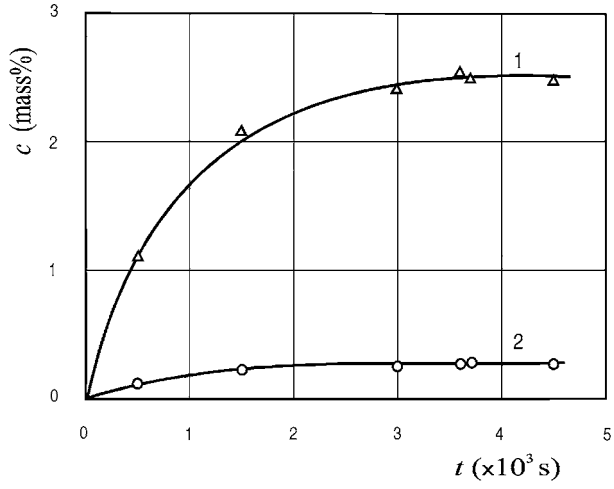

(a)

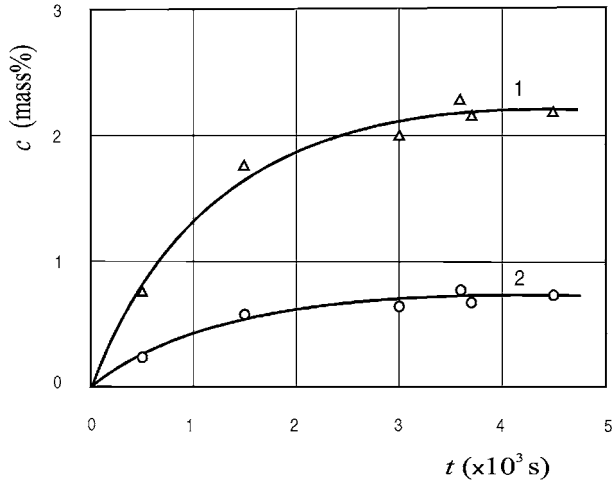

(b)

Figure 1 Contents of iron and chromium dissolved into liquid aluminium from the Fe–Cr alloys are plotted against time to determine the saturation concentrations, c_s. Temperature = 700°C, rotational speed $\omega = 54.0$ rad s^{-1}, $s/v = 27.5$ m^{-1}: (a) 90 mass% Fe–10 mass% Cr: 1, Fe; 2, Cr and (b) 75 mass% Fe–75 mass% Cr: 1, Fe; 2, Cr.

Note that the dissolution process of the Fe–Cr alloys in the aluminium melt appears to be non-selective. Indeed, the values for iron and chromium concentrations in the melt, obtained from mass-loss measurements on the assumption of non-selective dissolution of any Fe–Cr alloy in liquid aluminium, agree fairly well with those found by chemical analysis and electron probe microanalysis of Al–Fe–Cr alloys after the runs (see Table III).

It is worth mentioning that during crystallization of the Al–Fe–Cr melts two types of grains were formed in the cooled alloys, as seen in Figs 2–4. Some were large homogeneous grains typical of high-purity aluminium, while others were fine cellular ones characteristic of aluminium alloyed with transition metals. It might therefore seem that the Fe and Cr contents of those two regions would differ considerably. Surprisingly, this proved not to be the case. Though the EPMA data obtained using a small spot of 2 to 3 μm in diameter showed significant scatter, as expected, those determined with a round spot of about 50 μm in diameter or with a square spot of 100 × 100 μm^2, both covering

TABLE III Fe and Cr contents are listed as a function of time. The saturation concentration of iron and chromium in liquid aluminium can be determined from the data in this table. Temperature = 700°C, rotational speed $\omega = 54.0$ rad s^{-1}, $s/v = 27.5$ m^{-1}

		Elemental content (mass%)										
				CA						Averaged values of CA and EPMA		
		ML		US		UA		EPMA				
Run number	Time (s)	Fe	Cr	Fe	Cr	Fe	Cr	Fe	Cr	Fe	Cr	c_{Fe}: c_{Cr} in Al[a]
9s	500	1.10	0.12	1.13	0.10	1.08	0.14			1.10	0.12	9.2
10s	1500	2.06	0.22	2.03	0.25	2.11	0.20			2.08	0.23	9.0
1s	3000	2.23	0.25	2.46	0.26	2.50	0.25			2.48	0.25	9.9
2s	3600	2.48	0.27	2.61	0.27	2.50	0.28	2.50	0.28	2.54	0.28	9.1
4s	3700	2.49	0.28	2.57	0.29	2.45	0.27	2.47	0.27	2.50	0.28	8.9
3s	4500	2.31	0.26	2.59	0.27	2.50	0.29	2.62	0.29	2.57	0.29	8.9
11s	500	0.74	0.25	0.71	0.23	0.79	0.26			0.75	0.25	3.0
12s	1500	1.75	0.58	1.71	0.62	1.80	0.53			1.75	0.58	3.0
8s	3000	1.99	0.67	1.95	0.63	2.09	0.65			2.02	0.64	3.2
5s	3600	2.35	0.78	2.24	0.80	2.25	0.72	2.32	0.73	2.27	0.75	3.0
7s	3700	2.10	0.70	2.22	0.68	2.13	0.65	2.29	0.74	2.21	0.69	3.2
6s	4500	2.20	0.74	2.26	0.75	2.09	0.72	2.26	0.68	2.20	0.72	3.1

Note: ML = mass loss measurements, CA = chemical analysis, EPMA = electron probe microanalysis, US = United States, UA = Ukraine.
[a]Calculated from averaged values of CA and EPMA. The first six rows give the data for the dissolution of the 90 mass% Fe–10 mass% Cr alloy (C_{Fe}: $C_{Cr} = 9.0$); the next six rows for the 75 mass% Fe–25 mass% Cr alloy (C_{Fe}: $C_{Cr} = 3.0$).

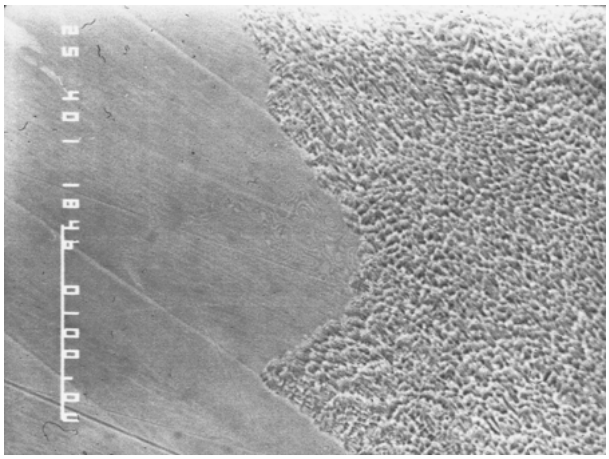

Figure 2 Secondary electron image of the transition zone between the homogeneous and cellular grains of an Al–Fe–Cr alloy obtained after the crystallization of the melt saturated with the alloy constituents in the course of determination of the saturation concentrations of iron and chromium for a 90 mass% Fe–10 mass% Cr alloy in liquid aluminium. Temperature = 700°C, rotational speed $\omega = 54.0$ rad s^{-1}, $s/v = 27.5$ m^{-1}, dipping time = 3600 s. Magnification ×400.

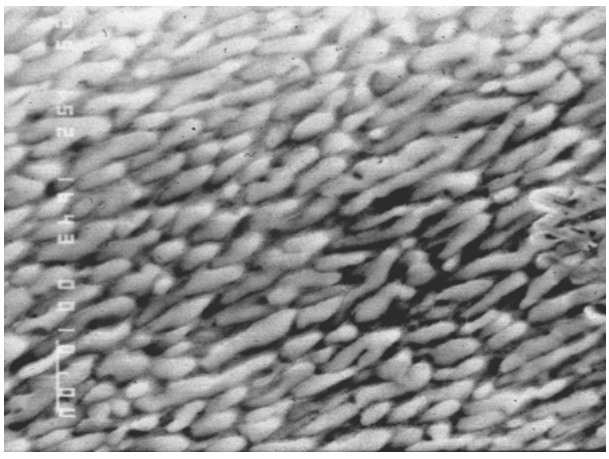

Figure 3 The cellular structure of Fig. 2 at a greater magnification of 1500.

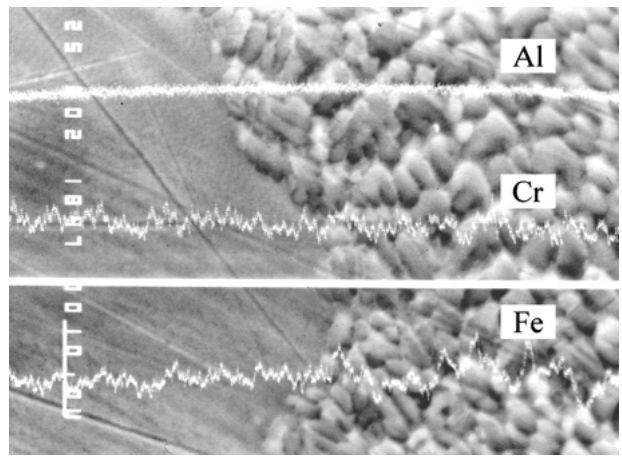

Figure 4 The concentration distribution of the elements in the transition zone between the homogeneous and cellular grains of an Al–Fe–Cr alloy (see Fig. 2). Magnification ×2000.

relatively large cross-sectional areas, gave almost identical values of Fe and Cr contents for both regions. This is readily seen in Table IV, where the average values of elemental concentrations are given. Measurements were made at random in both regions. The composition data provide evidence for the formation of a supersaturated aluminium solid solution in the homogeneous region since the solid-state solubilities of Fe and Cr in Al [3] are much less, even at the eutectic or peritectic temperature.

3.2. Determination of the dissolution rate constant

Besides the saturation concentration, c_s,another main characteristic of the dissolution process of a solid in a liquid is the dissolution rate constant, k. To obtain an accurate measure of k, the initials parts of the dissolution curves such as those shown in Fig. 1 were investigated in detail. The experimental data obtained

TABLE IV EPMA data for the Al–Fe–Cr alloys after the completion of the dissolution runs aimed at determining the saturation concentration, illustrating their compositional homogeneity, though structurally those alloys are not homogeneous (see Figs 2–4)

Content of Fe and Cr in the initial Fe–Cr alloy (mass%)			Elemental contents in the Al–Fe–Cr alloys (mass%)							
			Region of large homogeneous grains				Region of fine cellular grains			
			US		UA		US		UA	
Fe	Cr	Sample number	Fe	Cr	Fe	Cr	Fe	Cr	Fe	Cr
90	10	2s	2.54	0.28	2.53	0.27	2.47	0.30	2.47	0.27
		3s	2.71	0.29	2.59	0.29	2.60	0.29	2.61	0.31
75	25	5s	2.38	0.71	2.25	0.73	2.32	0.73	2.32	0.76
		6s	2.19	0.67	2.31	0.63	2.27	0.74	2.33	0.68

Note: US = United States, UA = Ukraine.

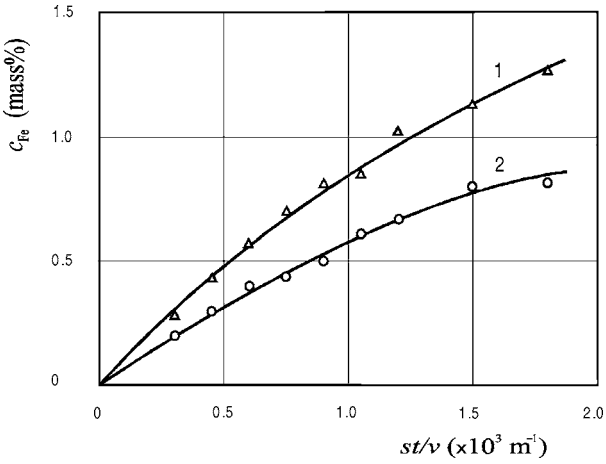

Figure 5 A plot of the concentration of iron, dissolved into liquid aluminium from the given Fe–Cr alloy, against st/v. Temperature = 700°C, rotational speed $\omega = 24.0$ rad s^{-1}, $s/v = 10.0$ m^{-1}. 1, 90 mass% Fe–10 mass% Cr alloy; 2, 75 mass% Fe–25 mass% Cr alloy.

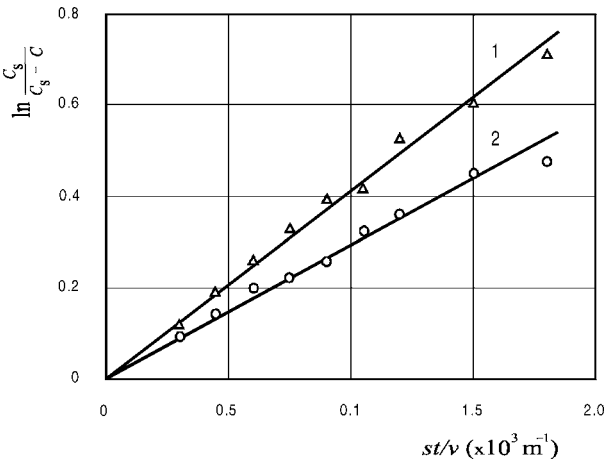

Figure 6 A plot of $\ln[c_s/(c_s - c)]$ against st/v for the data of Fig. 5.

are presented in Figs 5 and 6 and Tables V and VI. The linearity of a plot of $\ln [c_s/(c_s - c)]$ against time in Fig. 6 is evidence of the validity of Equations 2–4, which can thus be readily used to determine the dissolution rate constant of any Fe–Cr alloy in liquid aluminium. At an angular disc rotation speed of 24.0 rad s^{-1}, the value of k was found to be $(4.2 \pm 0.2) \times 10^{-5}$ m s^{-1} for a 90 mass% Fe–10 mass% Cr alloy and $(3.0 \pm 0.2) \times 10^{-5}$ m s^{-1} for a 75 mass% Fe–25 mass% Cr alloy.

TABLE V Determination of the dissolution rate constant for a 90 mass% Fe–10 mass% Cr alloy. Temperature = 700°C, rotational speed $\omega = 24.0$ rad s^{-1}, $s/v = 10.0$ m^{-1}

Time (s)	c_{Fe} (mass%)	c_{Cr} (mass%)	$\ln[c_s/(c_s - c)]$	k (×10^{-5} m s^{-1})
300	0.28	0.031	0.1188	4.0
450	0.43	0.048	0.1887	4.2
600	0.57	0.063	0.2588	4.3
750	0.70	0.078	0.3274	4.4
900	0.81	0.090	0.3916	4.3
1050	0.85	0.094	0.4155	4.0
1200	1.02	0.11	0.5242	4.4
1500	1.13	0.12	0.6014	4.0
1800	1.27	0.14	0.7093	3.9

The analysis of these and previous data shows that, for the same liquid-metal solvent, values of the dissolution rate constant rarely show a systematic change over the compositional range of a binary or multi-component alloy. This lack of systematic change is indicative of the complicated nature of the physicochemical interactions in the liquid state. Indeed, at a temperature of 700°C and a rotational speed $\omega = 24.0$ rad s^{-1}, $k = 3.8 \times 10^{-5}$ m s^{-1} for iron, 5.5×10^{-5} m s^{-1} for chromium and 6.5×10^{-5} m s^{-1} for nickel in their binary systems with aluminium (see [4]). Under the same conditions, $k = 5.9 \times 10^{-5}$ m s^{-1} for a 90 mass% Fe–10 mass% Ni alloy and 6.0×10^{-5} m s^{-1} for a 75 mass% Fe–25 mass% Ni alloy [6]. The dissolution rate constant of Fe–Ni alloys in liquid aluminium tends to decrease slightly with increasing time, while that of Fe–Cr alloys and an 18–10 stainless steel is indeed a constant, with a value of 4.8×10^{-5} m s^{-1} found for the latter [5].

In view of the larger value of the dissolution rate constant for chromium than for iron in their respective Al binary systems, it may seem surprising that k has a lower value for a 75 mass% Fe–25 mass% Cr alloy than for a 90 mass% Fe–10 mass% Cr alloy. The lower value for the former alloy is likely a result of the strong elemental interactions during their transition across the diffusion boundary layer into the bulk of liquid aluminium.

It is worth recalling that the concentration of the solute in the boundary layer in the vicinity of the surface of a solid phase is taken to be equal to its saturation concentration, c_s. For a 75 mass% Fe–25 mass% Cr alloy,

TABLE VI Experimental data for the dissolution kinetics of a 75 mass% Fe–25 mass% Cr alloy in liquid aluminium. Temperature = 700°C, rotational speed $\omega = 24.0$ rad s^{-1}, $s/v = 10.0$ m^{-1}

	c_{Fe} (mass%)		c_{Cr} (mass%)				
Time (s)	ML	CA	ML	CA	c_{Fe}:c_{Cr}	$\ln[c_s/(c_s - c)]$	k ($\times 10^{-5}$ m s^{-1})
300	0.20	0.21	0.07	0.06	3.5	0.0953	3.2
450	0.30	0.29	0.10	0.09	3.2	0.1887	3.2
600	0.40	0.39	0.13	0.13	3.0	0.2006	3.3
750	0.44	0.42	0.15	0.16	2.6	0.2231	3.0
900	0.50	0.51	0.17	0.16	3.2	0.2578	2.9
1050	0.61	0.64	0.20	0.18	3.5	0.3247	3.1
1200	0.67	0.68	0.22	0.24	2.8	0.3632	3.0
1500	0.80	0.74	0.26	0.24	3.1	0.4520	3.0
1800	0.82	0.79	0.27	0.26	3.0	0.4664	2.6

Note: ML = mass loss measurements, CA = chemical analysis.

c_s is 2.2 mass% Fe and 0.72 mass% Cr. Comparing those with the values of 2.5 mass% Fe and 0.72 mass% Cr for the respective Al binary systems, it can be concluded that for the 75 mass% Fe–25 mass% Cr alloy the ternary liquid solution, Al–Fe–Cr, is saturated with respect to both components (Fe and Cr). Therefore, iron and chromium atoms for this alloy must overcome a higher barrier in their transition into the melt than in the case of the 90 mass% Fe–10 mass% Cr alloy, for which the ternary liquid solution, Al–Fe–Cr, being saturated with respect to iron, is under-saturated with respect to chromium. This appears to slow down the rate of dissolution of a 75 mass% Fe–25 mass% Cr alloy in liquid aluminium, compared to that of a 90 mass% Fe–10 mass% Cr alloy.

3.3. Evaluation of the diffusion coefficient

For a rotating disc, the dissolution rate constant, k, is related to the diffusion coefficient, D, of the solute atoms across the diffusion boundary layer at the solid-liquid interface into the bulk of the liquid, the melt viscosity, ν, and the angular speed of rotation, ω, through the equation

$$k = 0.62 D^{2/3} \nu^{-1/6} \omega^{1/2} \quad (5)$$

proposed by Levich [8]. This equation allows the diffusion coefficient to be determined when the dissolution rate-constant is known, and *vice versa*. However, Equation 5 is only valid for Schmidt's numbers, Sc, exceeding 1000.

The Schmidt number is a dimensionless parameter equal to the ratio of the kinematic viscosity to the diffusion coefficient: $\mathrm{Sc} = \nu/D$. Usually, for liquid-metal melts $\mathrm{Sc} < 1000$. In such a case, a more accurate value of D can be obtained by using the following equation

$$k = 0.554 I^{-1} D^{2/3} \nu^{-1/6} \omega^{1/2} \quad (6)$$

in which the factor I is a (slight) function of the Schmidt number: $I = f(\mathrm{Sc})$. This equation was proposed by Kassner [9], and it is valid for $\mathrm{Sc} > 4$. In the range $10 < \mathrm{Sc} < 10^3$, typical of liquid-metals, the difference in the values of D determined using Equations 5 and 6 can be as high as 17% and as low as 3%.

To begin, an approximate value of the diffusion coefficient, D, was calculated using Equation 5. Just as in previous works [5, 6], the kinematic viscosity of the aluminium melt was taken to be constant over the full range of iron and chromium concentrations and equal to 4.8×10^{-7} m^2 s^{-1} [10]. Next, the Schmidt number, Sc, and the correction factor, I, were found. Finally, the value of the diffusion coefficient was calculated from Equation 6.

Following this procedure resulted in values of $D = 1.4 \times 10^{-9}$ m^2 s^{-1} for the 90 mass% Fe–10 mass% Cr alloy and $D = 0.9 \times 10^{-9}$ m^2 s^{-1} for the 75 mass% Fe–25 mass% Cr alloy. These diffusivity values are clearly averages for the concentration range 0–c_s. However, in view of the relative narrowness of this range, the concentration dependence of the diffusion coefficient may reasonably be expected to be insignificant.

The diffusivities characterize the rate of cooperative diffusion of iron and chromium atoms from the Fe–Cr alloys across the diffusion boundary layer into the bulk of the aluminium melt. For each Fe–Cr alloy, the iron and chromium diffusion coefficients thus found are identical in view of the non-selectivity of the dissolution process, even though in the respective binary systems Al–Fe and Al–Cr they differ considerably, being 1.2×10^{-9} m^2 s^{-1} for iron and 2.2×10^{-9} m^2 s^{-1} for chromium [4].

4. Conclusions

At 700°C, the dissolution process of the Fe–Cr alloys containing 10 and 25 mass% Cr in liquid aluminium is non-selective. Indeed, during dissolution, iron and chromium atoms pass into the bulk of the aluminium melt in that ratio in which they are present in an initial Fe–Cr alloy.

At an angular disk rotation speed of 24.0 rad s^{-1}, the dissolution rate constant was determined to be $(4.2 \pm 0.2) \times 10^{-5}$ m s^{-1} for a 90 mass% Fe–10 mass% Cr alloy and $(3.0 \pm 0.2) \times 10^{-5}$ m s^{-1} for a 75 mass% Fe–25 mass% Cr alloy. The slower dissolution of the latter alloy is likely a consequence of the strong mutual interaction of the alloy components during their transit across the diffusion boundary layer into the liquid aluminium melt. The extent of this interaction is dependent upon the content and the ratio of the alloy constituents in a saturated liquid-metal solution.

In view of the non-selectivity of the dissolution process with respect to Fe and Cr, the diffusion of the two

elements across the diffusion boundary layer into the bulk of the aluminium melt is characterized by a single value of the diffusion coefficient. This value is found to be 1.4×10^{-9} m^2 s^{-1} for the 90 mass% Fe–10 mass% Cr alloy and 0.9×10^{-9} m^2 s^{-1} for the 75 mass% Fe–25 mass% Cr alloy.

The data presented can be readily used to evaluate the thickness of dissolved Fe–Cr alloy during hot-dip aluminizing and the extent of saturation of the aluminium bath with the alloy constituents in the course of this process. The data can also be employed to evaluate the effect of dissolution on the growth rate of intermetallic layers at the interface between an iron-chromium alloy and molten aluminium.

Acknowledgements

This work was supported in part by the STCU grant no. 2028. The help of V. R. Sidorko, V. G. Khoruzha, K. A. Meleshevich, L. A. Duma, V. I. Kornilova, A. V. Samelyuk and V. M. Vereshchaka in conducting the experiments and carrying out the necessary analyses is acknowledged with gratitude.

References

1. L. I. MIRKIN, "Spravochnik po rentgenostrukturnomu analizu polikristallov" (Fizmatgiz, Moskwa, 1961) p. 458 (in Russian).
2. S. S. GORELIK, L. N. RASTORGUEV and YU. A. SKAKOV, "Rentgenograficheskiy i elektronno-opticheskiy analiz: prilozheniya" (Metallurgiya, Moskwa, 1970) p. 22 (in Russian).
3. T. B. MASSALSKI, J. L. MURRAY, L. H. BENNETT and H. BAKER (eds), "Binary Alloy Phase Diagrams," Vol. I (American Society for Metals, Metals Park, OH, 1986) p. 822.
4. V. I. DYBKOV, "Growth Kinetics of Chemical Compound Layers" (Cambridge International Science Publishing, Cambridge, 1998) Chapt. 5.
5. *Idem.*, *J. Mater. Sci.* **25** (1990) 3615.
6. *Idem.*, *ibid.* **28** (1993) 6371.
7. V. I. NIKITIN, "Fiziko-khimicheskiye yavleniya pri vozdeystvii zhidkikh metallov na tverdiye" (Atomizdat, Moskwa, 1967) Chapt. 1 (in Russian).
8. V. G. LEVICH, "Fiziko-khimicheskaya hidrodinamika" (Fizmatgiz, Moskwa, 1959) p. 77 (in Russian).
9. T. F. KASSNER, *J. Electrochem. Soc.* **114** (1967) 689.
10. E. S. LEVIN, *Izv. Akad. Nauk SSSR: Met.* **5** (1971) 72.

Received 12 September
and accepted 30 December 2002